THE JOURNAL OF BIOLOGICAL CHEMISTRY
Vol. 277, No. 5, Issue of February 1, pp. 3412–3418, 2002

Printed in U.S.A.

A Novel Binding Protein Composed of Homophilic Tetramer Exhibits Unique Properties for the Small GTPase Rab5*

Received for publication, July 5, 2001, and in revised form, October 3, 2001
Published, JBC Papers in Press, December 3, 2001, DOI 10.1074/jbc.M106276200

Kota Saito‡, Jun Murai‡, Hiroaki Kajiho, Kenji Kontani, Hiroshi Kurosu§, and Toshiaki Katada¶

From the Department of Physiological Chemistry, Graduate School of Pharmaceutical Sciences, University of Tokyo, Tokyo 113-0033, Japan

The small GTPase Rab family, which cycles between GTP-bound active and GDP-bound inactive states, plays an important role in membrane trafficking. Among them, Rab5 is involved in early endocytic pathway, and several Rab5-binding proteins have been identified as regulators or effectors to coordinate the docking and fusion processes of endocytic vesicles. We describe a novel binding protein exhibiting unique biochemical properties for Rab5. The Rab5-binding protein enhances GDP-GTP exchange reaction on Rab5 but preferentially interacts with its GTP-bound form. Gel filtration and immunoprecipitation analyses indicate that the Rab5-binding protein functions as a tetramer composed of anti-parallel linkage of two parallel dimers. These results suggest that the newly identified protein may function as an upstream activator and/or downstream effector for Rab5 in endocytic pathway. Possible roles of the quaternary structure have been discussed in terms of the Rab5-mediated signaling.

Recent studies (1–5) on endocytosis and exocytosis have indicated that vesicular transport between various membrane compartments is very complex and strictly regulated. Common steps in each pathway include membrane budding to form vesicles, their transport to a particular destination, and the docking and fusion of vesicles to their target membranes. Specificity of vesicular transport seems to be ensured by a number of factors including soluble *N*-ethylmaleimide-sensitive factor-1 attachment protein receptor molecules and the small GTPase Rab family. The proper pairing and complex formation between target and vesicular soluble *N*-ethylmaleimide-sensitive factor-1 attachment receptor proteins are responsible for the stable attachment of the vesicles to the target membranes. On the other hand, the small GTPase Rab family, which cycles between GTP-bound active and GDP-bound inactive states, appears to be involved in the membrane-tethering step in concert with their binding proteins (1–5). However, the molecular mechanisms underlying the coupling of these processes are not fully understood.

At present, more than 40 members of the Rab family have been identified, and several members appear to be involved in each specific step of endocytic pathways (6–12). Rab5 has been principally implicated in the fusion process of endosomes and is known as a rate-limiting factor for homotypic endosome fusion (10, 13). GDP-bound Rab5 is mostly abundant in endosome membranes and is extracted by GDI[1] (10, 14–17). Recent studies have revealed that p38 activates the extraction of Rab5 by phosphorylating GDI (18). After extraction, GDI-Rab5 complex is delivered to the appropriate target membrane where Rab5 is reloaded via a yet unidentified GDI displacement factor (19, 20). GDP-Rab5 in the target membrane is subsequently activated by guanine nucleotide exchange factors (GEF). As one of Rab5 stimulators, the 60-kDa Rabex-5, which is homologous to the yeast vacuolar protein-sorting 9 (Vps9) protein, has been identified (21, 22). GTP-Rab5 then interacts with several Rab5 effectors such as phosphatidylinositol 3-kinases, Rabaptin-5, EEA-1, and Rabenosyn-5 to coordinate endosome fusion (23–27).

Recently, Rab5 has also been implicated in membrane receptor internalization (28–30) and in organelle association with or movement upon cytoskeletal networks (31). The GTP form of Rab5 appeared to be required for sequestering ligands into clathrin-coated vesicles in the endocytosis of the ligand-receptor complexes. Moreover, Rab5 may directly interact with a motor protein to regulate the motility of early endosomes on microtubules. These results suggest that the activation of Rab5 should be coordinated with the receptor activation by ligands, because sequestration of receptor is tightly connected with its activation.

In the present study, we report a novel Rab5-binding protein, RIN2, that has a sequence similar to the recently reported Ras-mediated Rab5 stimulator, RIN1 (32). RIN2 displays unique biochemical properties compared with well known GEFs for small GTPases. RIN2 preferentially interacts with the GTP form of Rab5 rather than the GDP form, although it enhances the guanine exchange reaction on Rab5. Moreover, gel filtration and immunoprecipitation analyses suggest that RIN2 could form a tetramer composed of anti-parallel linkage of two parallel dimers. These results suggest that RIN2 may function as an upstream activator and/or downstream effector for Rab5 in the endocytic pathway.

* This work was supported in part by research grants from the "Research for the Future" Program of the Japan Society for the Promotion of Science JSPS-RFTF 96L00505 and the Scientific Research Funds of the Ministry of Education, Culture, Sports, Science and Technology of the Japanese Government. The costs of publication of this article were defrayed in part by the payment of page charges. This article must therefore be hereby marked "*advertisement*" in accordance with 18 U.S.C. Section 1734 solely to indicate this fact.

The nucleotide sequence reported in this paper has been submitted to the DDBJ/GenBank™/EBI Data Bank with accession numbers AB060338 and AB060339.

‡ Both authors contributed equally to this work.

§ Present address: Howard Hughes Medical Institute Research Laboratories, the University of Texas Southwestern Medical Center, 5323 Harry Hines Blvd., Dallas, TX 75390-9050.

¶ To whom correspondence should be addressed: Dept. of Physiological Chemistry, Graduate School of Pharmaceutical Sciences, University of Tokyo, Hongo, Tokyo 113-0033, Japan. Tel.: 81-3-5841-4750; Fax: 81-3-5841-4751; E-mail: katada@mol.f.u-tokyo.ac.jp.

[1] The abbreviations used are: GDI, guanine nucleotide dissociation inhibitor; CHAPS, 3-[(3-cholamidopropyl)dimethyl-ammonio]-1-propanesulfate; DTT, dithiothreitol; GEF, guanine nucleotide exchange factor; GTPγS, guanosine 5′-(γ-thio)triphosphate; SH2, Src homology 2; WT, wild type; RA, Ras association.

EXPERIMENTAL PROCEDURES

Materials—Monoclonal anti-FLAG(M2) and anti-Myc (9E10) antibodies were purchased from Sigma. All other reagents were from commercial sources and of analytical grade.

Yeast Two-hybrid Assay—A yeast two-hybrid screen was performed according to the method described previously (33) utilizing the Matchmaker two-hybrid system (CLONTECH Laboratories). A human leukocyte cDNA library in the pGAD10 vector was screened with Rab5b/Q79L as bait, which was inserted into pGBT9. The cDNA library and bait were co-transformed into the yeast two-hybrid strain HF7c by using a lithium acetate-based method. Positive clones grown on His^- medium were selected for activation of HIS3 reporter gene, and β-galactosidase assay was performed as described previously (34, 35). The 1575-bp human cDNA encoding the partial sequence of RIN3 (see "Results") has been submitted to the DDBJ/EMBL/GenBank™ data bases under accession number AB060338. Deletion mutants of RIN2 (see "Results") were constructed using a PCR-based strategy. PCR products encoding amino- and carboxyl-terminal truncations of RIN2 were subcloned into pGBT9 in-frame with the GAL4 DNA-binding domain. The two-hybrid vectors obtained were co-transformed into the yeast host strain Y190 or SFY526. Transformed colonies were replated on tryptophan- and leucine-deficient medium.

Cloning of the Full-length RIN2 cDNA—Extension of JC265 cDNA was performed by 5′-rapid amplification of cDNA end-PCR to a human brain Marathon Ready cDNA (CLONTECH), according to the manufacturer's protocols. To amplify the complete coding sequence of the cDNA, an oligonucleotide corresponding to the upstream sequence of the ATG initiation codon was selected. The 5′-rapid amplification of cDNA end-PCR fragment was purified and subcloned into pGEM-T (Promega) and sequenced. The 2685-bp cDNA encoding RIN2 has been submitted to the DDBJ/EMBL/GenBank™ Data Bank under accession number AB060339.

Northern Blot Analysis—A human multiple tissue RNA blot containing various tissues (2 μg/lane of poly(A) RNA) was obtained from CLONTECH Laboratories. Total cellular RNAs were also prepared from various cell lines using TRIZOL reagent (Invitrogen). Poly(A) RNAs were separated from the total RNA by a Poly(A)Tract mRNA Isolation System III (Promega), according to the manufacturer's protocols. The isolated poly(A) RNAs (2 μg) were denatured by heating at 65 °C for 5 min in 2.2 M formaldehyde and 50% (v/v) formamide and size-fractionated by 1.2% agarose gel containing 2.2 M formaldehyde. The RNAs were transferred directly to nylon membrane filters. An [α-^{32}P]dCTP-labeled fragment corresponding to the amino acid sequence 213–570 of RIN2 was hybridized to the filters overnight at 65 °C in an ExpressHyb Solution (CLONTECH), and the filters were washed and subjected to autoradiography.

Production of Recombinant Proteins—COS-7 or HeLa cells were transfected with pCMV5 containing the cDNA of FLAG-tagged RIN2. Transfected cells were washed twice with phosphate-buffered saline and solubilized with buffer A consisting of 40 mM Hepes-NaOH (pH 7.4), 75 mM NaCl, 15 mM NaF, 1 mM Na_3VO_4, 10 mM $Na_4P_2O_7$, 2 mM EDTA, 1 μg/ml leupeptin, 2 μg/ml aprotinin, 1% Nonidet P-40 by vortexing. After gently rotated for 15 min at 4 °C, lysates were centrifuged at 15,000 rpm for 15 min at 4 °C. Supernatants were precleared with 20 μl of anti-mouse IgG-agarose resin (50% slurry, American Qualex Inc.) and immunoprecipitated with 10 μl of the agarose resin that had been conjugated with 0.5 μg of the anti-FLAG monoclonal antibody. The resin was washed three times with 1 ml of 20 mM Tris-HCl (pH 7.5), 150 mM NaCl, and 1% (w/v) Nonidet P-40, and three more times with a buffer consisting of 50 mM Hepes-NaOH (pH 7.5), 100 mM NaCl, 7.7 mM $MgCl_2$, 2 mM EDTA, and 0.1% (w/v) Nonidet P-40. FLAG-tagged RIN2 was eluted from the resin with the same buffer containing 1 mg/ml of FLAG peptide.

Prenylated Rab5b was purified from baculovirus-infected Sf9 cells according to the method described previously (36), unless 10 μM GDP was added to each buffer. To prepare GTPγS and GDP forms of Rab5b, the purified protein was incubated with the nucleotides (250 μM) at 30 °C for 45 min in 11.2 mM Tris-HCl (pH 8.0), 50 mM Hepes-NaOH (pH 7.5), 110 mM NaCl, 0.5 mM DTT, 0.27% (w/v) CHAPS, 5 mM EDTA, and 2.2 mM $MgCl_2$. The reaction was terminated by adding $MgCl_2$ to the final concentration of 10 mM.

Assays for GTPγS Binding and in Vitro Association between Rab5b and RIN2—[^{35}S]GTPγS binding assay was performed by the filter method as described previously (16). Prenylated Rab5b (10 nM) was incubated with 25 nM [^{35}S]GTPγS (50,000 cpm/pmol) at 30 °C for the indicated times with or without FLAG-tagged RIN2 purified from the transfected HeLa cells in a reaction mixture (50 μl) consisting of 20 mM Tris-HCl (pH 8.0), 62.5 mM NaCl, 0.5 mM DTT, 500 nM GDP, 0.36% (w/v) CHAPS, 5 mM EDTA, and 15 mM $MgCl_2$, 0.3 mg/ml FLAG peptide.

To assay the association between Rab5 and RIN2, the GDP- or GTPγS-bound Rab5b was incubated with the resin (10 μl) conjugating FLAG-RIN2 at 25 °C for 60 min in 0.25 ml of 50 mM Hepes-NaOH (pH 7.4), 10 mM $MgCl_2$, 5 mM EDTA, 0.5 mM DTT, 100 mM NaCl, and 0.1% (w/v) Nonidet P-40. The agarose resin was washed four times with a buffer (500 μl) consisting of 50 mM Tris-HCl (pH 8.0), 100 mM NaCl, 7 mM $MgCl_2$, 2 mM EDTA, and 0.2% (w/v) Nonidet P-40. Proteins were eluted from the resin with 30 μl of the same buffer containing 1 mg/ml FLAG peptide. After centrifugation, 24 μl of the supernatant was mixed with 8 μl of 4× SDS sample buffer, boiled for 5 min, and followed by SDS-PAGE. The concentrations of acrylamide used to separate FLAG-RIN2 and Rab5b are 8 and 15%, respectively. Immunoblotting was performed with the anti-FLAG monoclonal antibody and the anti-Rab5b polyclonal antibody A-20 (Santa Cruz Biotechnology), respectively.

Immunoprecipitation and Gel Filtration Analyses—Transfected HeLa cells were washed twice with phosphate-buffered saline and solubilized with buffer A and then diluted with buffer A not containing Nonidet P-40 to lower the concentration of Nonidet P-40 to 0.5%. After gently rotated for 15 min at 4 °C, lysates were centrifuged at 15,000 rpm for 15 min at 4 °C. Supernatants were precleared with Sepharose 4B resins (Amersham Biosciences) and immunoprecipitated with anti-FLAG M2-agarose beads (Sigma) or anti-Myc 9E10 (Sigma)-conjugating anti-IgG-agarose resin by gently rotating for 2 h at 4 °C. The beads, after washing three times with 0.5 ml of Tris-buffered saline, 0.1% Nonidet P-40 were washed three more times with buffer B consisting of 75 mM Tris-HCl (pH 7.5), 1 mM EDTA, 100 mM NaCl, 0.2% Nonidet P-40. For SDS-PAGE analysis, the beads were mixed with 24 μl of buffer B and 12 μl of 4× sample buffer and boiled for 2 min. The samples were resolved by SDS-PAGE, and immunoblotting was performed with anti-FLAG and anti-Myc antibodies.

For gel filtration analysis, the beads were washed six times with 0.5 ml of buffer C consisting of 25 mM Tris-HCl (pH 7.5), 150 mM NaCl, 0.2% CHAPS and subsequently eluted with 0.2 ml of buffer C containing 1 mg/ml FLAG peptide by gently vortexing for 1 h at 4 °C. The eluted fraction was diluted with an equal volume of buffer C and applied to a Superdex 200 column (HR 10/30 Amersham Biosciences) that had been equilibrated with buffer C. Elution was carried out at room temperature at a flow rate of 0.5 ml/min with a fraction volume of 0.25 ml. The fractions were concentrated by precipitation with 10% (final) trichloroacetic acid and subjected to SDS-PAGE and silver staining. The fractions were also analyzed by SDS-PAGE and immunoblotted with anti-FLAG antibody. The elution profile of the column was calibrated with the sizing standards (Oriental Yeast Co. Ltd.) of glutamate dehydrogenase (290 kDa), lactate dehydrogenase (142 kDa), enolase (67 kDa), adenylate kinase (32 kDa), and cytochrome *c* (12.4 kDa).

RESULTS

Complementary DNA Cloning of Rab5-binding Proteins—We searched for binding proteins for GTP-bound form of Rab5 in a yeast two-hybrid screening system. A human leukocyte cDNA library was screened with the GTPase-deficient mutant Rab5b/Q79L. Screening of 5×10^7 transformants yielded five positive clones that strongly interacted with Rab5b/Q79L. One of the five clones, tentatively termed as HK281, consisted of a 1575-base pair (bp) cDNA encoding 525 amino acids. Further analysis of HK281, together with the isolation of its full-length sequence, is currently under investigation in our laboratory and will be described elsewhere as RIN3.

Homology search using data base with FASTA and BLAST revealed that HK281 has sequence similarity with two independent cDNA clones, Ras-interaction/interference 1 (RIN1) and a partially identified RIN1-raleted JC265 (37, 38). Full-length sequence of JC265 was obtained by 5′-rapid amplification of cDNA ends, with an initiation codon based on the Kozak consensus sequence. The total cDNA encodes an 895-amino acid protein, in which the originally isolated fragment of JC265 corresponds to the amino acid sequence 425–895. This protein contained an SH2 domain, two proline-rich motifs, a Vps9 domain, and Ras association (RA) domain from the amino terminus (see Fig. 3*A*). Because this protein has similar domain architecture and high sequence homology to RIN1, it was

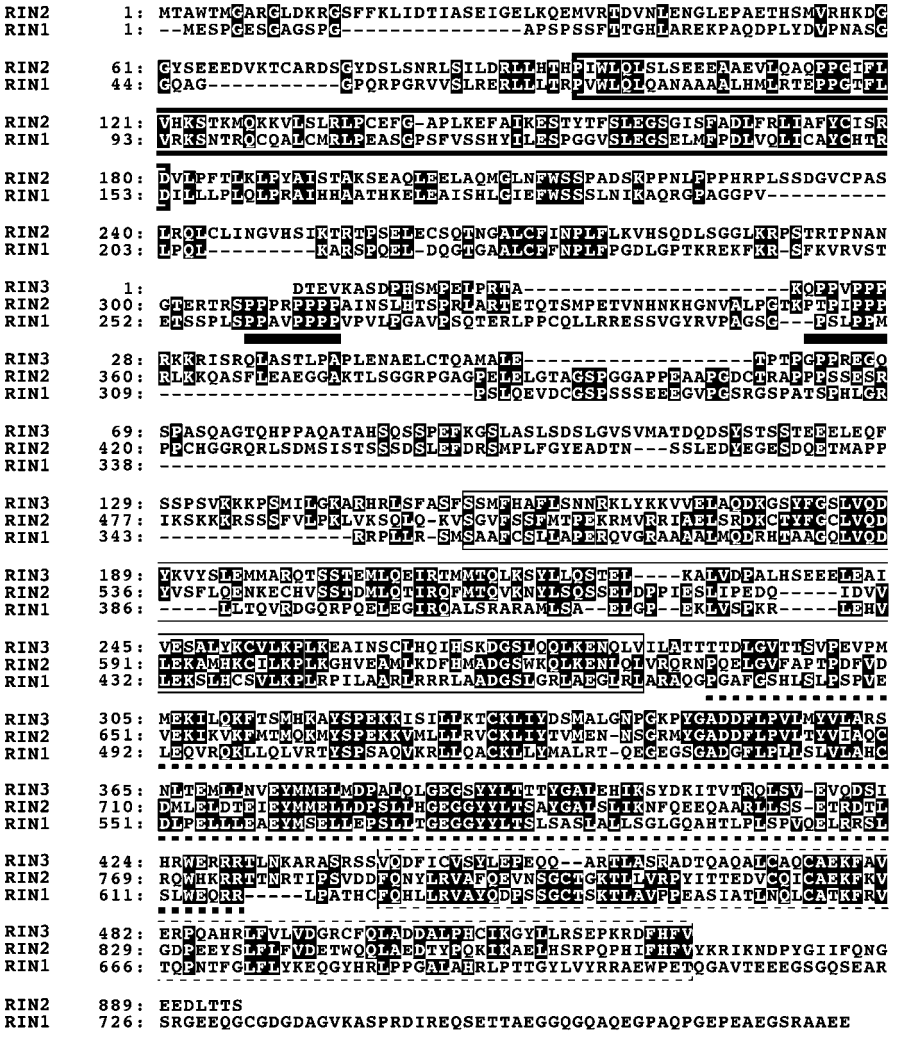

FIG. 1. **Amino acid sequence alignments of RIN family.** The sequence alignment among HK281 (partial RIN3), RIN2, and RIN1 (DDBJ/EMBL/GenBank™, accession number L36463) is shown in the single-letter amino acid code. The *numbers* represent positions of the amino acid residues. *Block boxes* indicate identical amino acids. The SH2 domain is *boxed* with a *bold line*. Proline-rich motif is *underlined* with a *bold line*. The RH domain is *boxed*. The Vps9 domain is *underlined* with a *dashed line*. The RA domain is *boxed* with a *dashed line*.

henceforth referred to as RIN2. Fig. 1 shows the amino acid alignment of RIN1, RIN2, and the partial sequence of RIN3 (clone HK281).

Expression of RIN2 mRNA in Human Tissues and Cells—The distribution of RIN2 mRNA in human tissues was examined by Northern blot analysis with a radiolabeled probe containing a 1.07-kb coding sequence of RIN2. As shown in Fig. 2*A*, a 5.1-kb transcript was the most abundant in human heart and kidney with the lowest expression level in the spleen and peripheral blood cells. Furthermore, the 5.1-kb mRNA was also present in human cell lines, HeLa and N-1321 astrocytoma cells, but not in leukemic cell lines, Jurkat and THP-1 cells (Fig. 2*B*). The expression pattern of RIN2 mRNA was different from those of other RIN family proteins, because RIN1 has been reported to be abundant in brain tissues (39) and RIN3 displayed rather ubiquitous distribution including blood cells.[2]

Specificity of the Interaction between Rab5 and RIN2—We further examined the interaction between RIN2 and Rab5b in the yeast two-hybrid system. RIN2 sufficiently interacted with Rab5b/WT, in addition to the constitutively active form Rab5b/Q79L (Fig. 3*B*). However, the dominant negative form Rab5b/S34N exhibited weak interaction with RIN2. Other members of the Rab family including Rab4, Rab7, Rab9, and Rab11 failed to interact with RIN2. Although Ha-Ras was reported to interact with RIN1 in the yeast two-hybrid system (39), neither the wild type (Ha-Ras/WT) nor the active form (Ha-Ras/G12V)

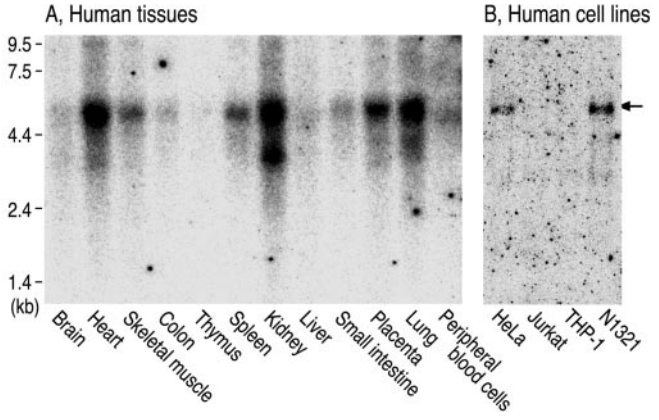

FIG. 2. **Northern blot analysis of RIN2.** The probe was labeled by random priming and hybridized to a human multiple tissue RNA blot containing poly(A) mRNA from various human tissues (*A*) and to a nylon membrane to which poly(A) mRNA from the human cell lines of HeLa, Jurkat, THP-1, and 1321N1 had been transferred (*B*). Two μg of poly(A) mRNA were loaded in each lane.

associated with RIN2 under our assay conditions.

To identify the Rab5-binding region, various deletion mutants of RIN2 were generated and further analyzed in the two-hybrid system (Fig. 3*C*). In addition to the full-length RIN2, its carboxyl-terminal half-sequence (residues 497–895) strongly interacted with Rab5b. Such strong interaction was completely abolished by further deletion of its amino-terminal

[2] H. Kajiho and K. Saito, unpublished data.

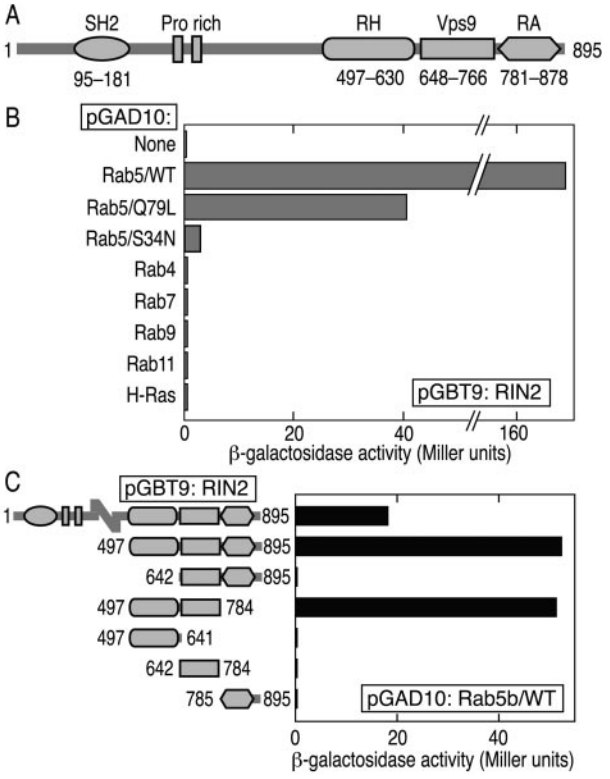

FIG. 3. **Interaction of Rab5b with RIN2 in yeast two-hybrid system.** *A*, RIN2 contains the SH2 domain, two proline-rich motifs, the RH domain, the Vps9 domain, and the RA domain. The numbers represent the amino acid residues. *B*, the interaction between the full-length RIN2 and various forms of Rab5b or other members of small GTPase family was analyzed in the yeast two-hybrid assay as described under "Experimental Procedures." *C*, the amino- and carboxyl-terminal deletion mutants of RIN2 and Rab5b/WT were inserted into pGBT9 and pGAD10 vectors, respectively, and transformed into SFY526 cells. β-Galactosidase activity was assayed as described under "Experimental Procedures."

region (RH domain, see "Discussion"), but not changed by the elimination of RA domain. RH, Vps9, or RA domain alone failed to interact with Rab5b. Thus, the sequence 497–784 of RIN2, which contains both RH and Vps9 domains, appeared to be minimally required for Rab5 binding.

Unique Biochemical Properties of RIN2—We next investigated how the nucleotide-bound state of Rab5 exerts its influence on the interaction with RIN2 in an *in vitro* binding assay. FLAG-tagged RIN2 immobilized to resins was incubated with GDP- or GTPγS-bound form of Rab5b. The Rab5 binding was estimated by immunoblotting with an anti-Rab5b antibody. As shown in Fig. 4 (*lanes 3* and *4*), the GTPγS form of Rab5b more efficiently bound to RIN2 than did its GDP form, in accordance with the results in the yeast two-hybrid system (see Fig. 3*B*).

Because RIN2 contained the Vps9 domain (the amino acid sequence 648–766) conserved in other characterized GEFs for Rab5 (21, 22), we also investigated whether this binding protein has a GEF activity for Rab5. For the analysis, [^{35}S]GTPγS-binding experiments were performed with FLAG-tagged RIN2 and prenylated Rab5b that had been purified from transfected HeLa cells and baculovirus-infected Sf9 cells, respectively (Fig. 5*A*). As shown in Fig. 5*B*, [^{35}S]GTPγS binding to the purified Rab5b was very slow at the physiological concentration (millimolar order) of Mg^{2+}, which resulted from slow GDP dissociation from the small GTPase. Under these conditions, RIN2 markedly accelerated GTPγS binding to Rab5b, although the binding protein itself had no detectable GTPγS binding activity. Interestingly, the binding accelerated by RIN2 was apparently maximal during the first 5 min, and further incubation

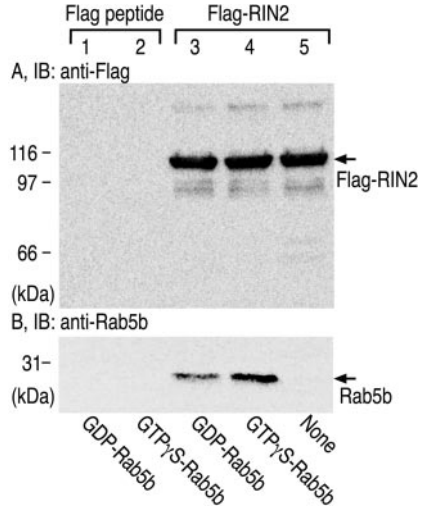

FIG. 4. ***In vitro* binding of Rab5b to RIN2.** FLAG-tagged RIN2 (*lanes 3* and *4*) and FLAG peptide alone (*lanes 1* and *2*) were expressed in COS-7 cells and subjected to immunoprecipitation with anti-FLAG antibody-conjugated resin. The precipitated resin was washed and incubated with GDP- (*lanes 1* and *3*) or GTPγS-bound (*lanes 2* and *4*) Rab5b. Proteins bound to the resin were separated by SDS-PAGE and immunoblotted (*IB*) with anti-FLAG (*A*) and anti-Rab5b (*B*) antibodies.

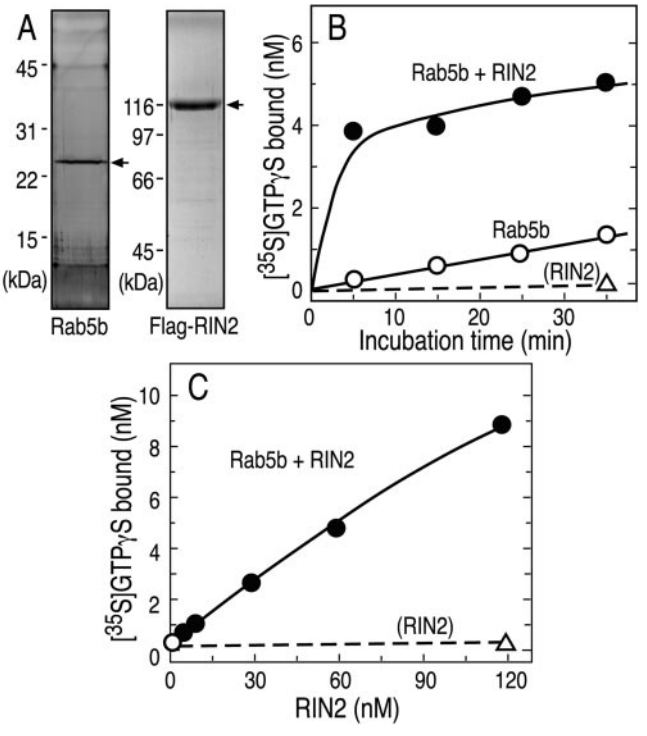

FIG. 5. **Effect of RIN2 on GTPγS binding to Rab5b.** *A*, prenylated Rab5b (*left*) and FLAG-tagged RIN2 (*right*) that had been purified as described under "Experimental Procedures" were analyzed by SDS-PAGE and stained with silver and Coomassie Brilliant Blue, respectively. *B*, Rab5b (10 nM) was incubated with [^{35}S]GTPγS at 30 °C for the indicated times in the presence or absence of 60 nM RIN2, and [^{35}S]GTPγS binding to Rab5b was measured. *C*, Rab5b (10 nM) was incubated with [^{35}S]GTPγS at 30 °C for 15 min in the presence of the indicated concentrations of RIN2.

did not stimulate guanine nucleotide exchange reaction on Rab5b (Fig. 5*B*). The GTPγS binding to Rab5b was dependent on the concentration of RIN2, and the maximum level reached to the stoichiometric amount (10 nM) of the small GTPase (Fig. 5*C*). These properties observed in RIN2 are quite different from those of other characterized GEFs, which act catalytically on the small GTPases (see "Discussion").

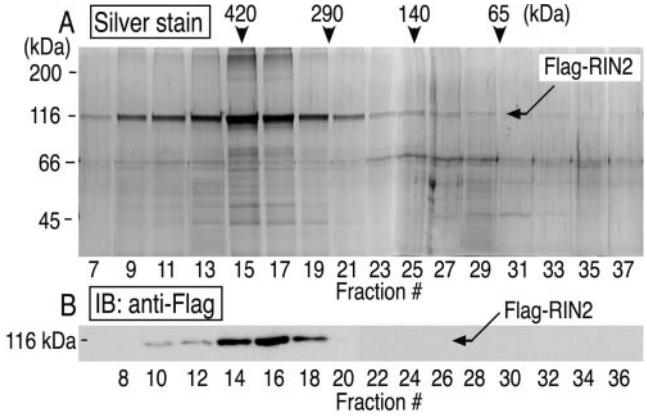

FIG. 6. **Tetramer formation of RIN2.** FLAG-tagged RIN2 was purified from HeLa cells and applied to a Superdex 200 gel filtration column as described under "Experimental Procedures." The elution position was compared with those of the globular size markers (*arrowheads*). *A*, the fraction (0.5 ml) eluted from the column was analyzed by SDS-PAGE, and proteins were stained with silver. *B*, the fraction was analyzed by SDS-PAGE and immunoblotted (*IB*) with the anti-FLAG antibody. *Arrows* indicate the position of FLAG-tagged RIN2.

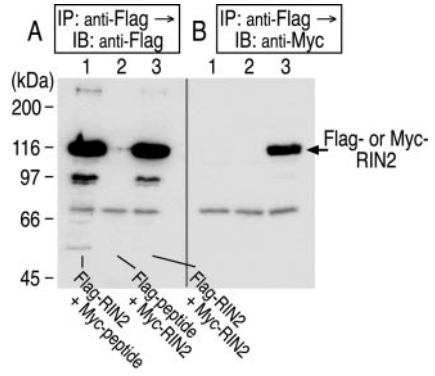

FIG. 7. **Self-interaction of full-length RIN2.** FLAG-tagged RIN2 *plus* Myc peptide (*lane 1*), FLAG peptide *plus* Myc-tagged RIN2 (*lane 2*), and FLAG-tagged *plus* Myc-tagged RIN2 (*lane 3*) were co-expressed in HeLa cells and subjected to immunoprecipitation (*IP*) with anti-FLAG-agarose beads. The precipitants were analyzed by SDS-PAGE and immunoblotted (*IB*) with anti-FLAG (*A*) and anti-Myc (*B*) antibodies. *Arrow* indicates the position of FLAG- or Myc-tagged RIN2.

Gel Filtration Analysis of RIN2—When FLAG-tagged RIN2, purified from transfected HeLa cells, was analyzed by immunoblotting with an anti-FLAG antibody, we noticed a faint band of more than 200 kDa, in addition to a band corresponding to the RIN2 monomer of 116 kDa (see Fig. 4*A*, *lanes 3–5*). Because this band was not detected in control cells (Fig. 4*A*, *lanes 1* and *2*), we speculated that RIN2 might form a multicomplex. To investigate this possibility, FLAG-tagged RIN2 was applied to a gel filtration column, and fractions eluted from the column were analyzed by SDS-PAGE and immunoblotting with the anti-FLAG antibody. As shown in Fig. 6, FLAG-tagged RIN2 was eluted at an apparent molecular weight of ~420,000. There was no detectable protein stoichiometrically associated with RIN2. These results indicate that RIN2 could self-interact to form a homophilic tetramer.

Tetramer Formation of RIN1 Composed of Anti-parallel Linkage of Two Parallel Dimers—To investigate the structural features of RIN2, various forms of FLAG and Myc epitope-tagged RIN2 were expressed in HeLa cells. We first checked whether the self-interaction of full-length RIN2 could be detected with this system. As shown in Fig. 7, Myc-tagged RIN2 was efficiently co-immunoprecipitated with the anti-FLAG antibody when co-expressed with FLAG-RIN2 (Fig. 7*B*, *lane 3*). FLAG-RIN2 was also detected when Myc-tagged RIN2 was precipitated with the anti-Myc antibody (data not shown). These results support the idea that RIN2 forms a homophilic tetramer.

Further experiments were performed with Myc-tagged full-length RIN2 and FLAG-tagged deletion mutants. Under the conditions that each of the FLAG-tagged deletion mutants could be detected with the anti-FLAG antibody (data not shown), the existence of Myc-tagged full-length RIN2 was analyzed (Fig. 8*B*). Deletion of carboxyl-terminal RH, Vps9, and RA domains and amino-terminal SH2 domain did not diminish the self-interaction (Fig. 8*B*, *lanes 1–3*), whereas further deletion of amino-terminal proline-rich motifs completely abolished the interaction (*lane 4*). Moreover, carboxyl-terminal Vps9 and RA domains also interacted with full-length RIN2, although the interaction was rather weak (*lanes 5* and *6*).

We also investigated whether the amino- and carboxyl-terminal parts of RIN2 can interact with themselves or with each other. As shown in Fig. 8*C*, the region between the SH2 domain and proline-rich motifs was responsible for the amino-terminal self-interaction (*lanes 1–4*). The carboxyl-terminal part of RIN2 also interacted with itself, and the interacting region was assigned to the carboxyl-terminal RA domain (*lanes 5–10*), although the RH domain fairly interacted with itself (*lane 8*). These results indicate that RIN2 might form parallel complexes. To clarify whether RIN2 might form anti-parallel complexes, the interaction between the amino and carboxyl termini was further investigated. As shown in Fig. 8*D*, the amino- and carboxyl-terminal interaction appeared to be existent. The region between SH2 domain and proline-rich motifs was required for interaction with carboxyl-terminal RH and Vps9 domains. These results indicate that RIN2 might also form anti-parallel complexes.

DISCUSSION

Structural Features of the RIN Family Rab5-binding Proteins—In the present study, we have identified a novel Rab5-binding protein, RIN2, consisting of 895 amino acids. RIN2 contains SH2 domain, two proline-rich motifs, Vps9 domain, and RA domain, which have also been conserved in RIN1 (39). Moreover, another Rab5-binding protein, RIN3, partially identified in this study seems to belong to this family, although its amino-terminal sequence has not been determined yet. The alignment of the three proteins allowed us to depict a conserved 100-amino acid sequence in the central region of this family. We termed this conserved region as RH domain (for RIN Homology).

This RH domain, together with Vps9 domain, constituted a region necessary for Rab5 binding (Fig. 3*B*). On the other hand, the carboxyl-terminal RA domain of RIN2 was not responsible for the Rab5 binding, consistent with recent report for RIN1 (32). Although the RA domain of RIN1 has been identified as a Ras-binding region (39), we could not observe the significant interaction between full-length RIN2 and Ha-Ras under the present conditions (Fig. 2). Another significant feature different from RIN1 is that both RIN2 and RIN3 have an insertion of an extra 120-amino acid sequence between Pro-rich motif and RH domain. The extra sequence exhibits the lowest homology between RIN2 and RIN3.

Homophilic Tetramer Formation of RIN2—In this report, we show the evidence that RIN2 exists as a tetramer composed of anti-parallel linkage of two parallel dimers. First, RIN2 was eluted at ~420 kDa in gel filtration column chromatography, approximately four times as large as the apparent molecular mass of the monomer (Fig. 6). Second, self-interaction was observed between different epitope-tagged forms of full-length RIN2 (Fig. 7). Third, amino- and carboxyl-terminal RIN2 fragments could dimerize homogeneously and heterogeneously

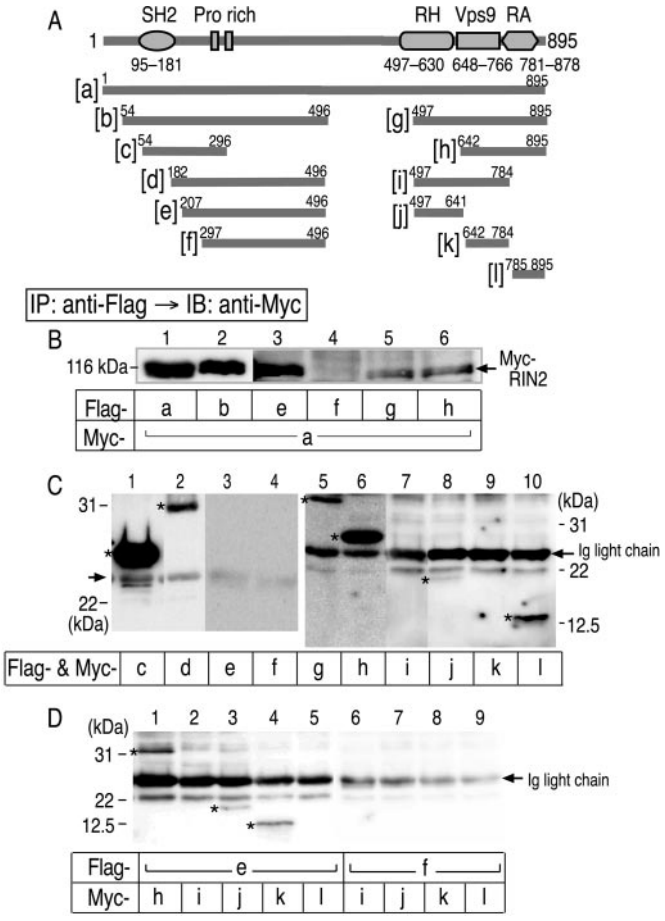

FIG. 8. **Analysis of self-interacting regions on RIN2.** *A*, schematic representation of RIN2 deletion mutants used in this experiment. RIN2 contains SH2 domain, two proline-rich motifs, RH domain, Vps9 domain, and RA domain. The *letters in brackets* correspond to the lane definitions in *B–D*. *B–D*, Myc-tagged full-length RIN2 and each of the FLAG-tagged deletion mutants (*B*), a pair of Myc-tagged and FLAG-tagged deletion mutants (*C*), and FLAG-tagged amino-terminal and Myc-tagged carboxyl-terminal mutants (*D*) were co-expressed in HeLa cells and immunoprecipitated (*IP*) by anti-FLAG agarose beads. The precipitants were analyzed by SDS-PAGE and immunoblotted (*IB*) with anti-Myc antibody. *B*, *arrow* indicates the position of Myc-tagged RIN2. *C* and *D*, *asterisks* indicate Myc-tagged deletion mutants immunoprecipitated with FLAG-tagged mutants. *Arrows* indicate the position of Ig light chain.

(Fig. 8). Based on these results, we propose the quaternary structure of RIN2 as indicated in Fig. 9.

Recent reports indicate that several proteins implicated in early endocytic pathways form homo-multimeric complexes. For example, Eps15, a phosphorylation substrate of the epidermal growth factor receptor kinase forms a tetramer consisting of parallel and anti-parallel dimers (40, 41), which resembles the proposed structure of RIN2. As for Rab5 effectors, Rabaptin-5 and EEA-1 has been respectively shown to form dimers (42, 43). Moreover, it is suggested that Rab5 can be dimerized depending on the GTP-bound conformation (44). RIN2 may function as a component of early endocytic machinery in the form of homophilic complex, in coordination with other oligomeric complexes (45).

Unique Properties of RIN2 for Rab5—In the present study, we revealed that RIN2 stimulates a guanine nucleotide exchange reaction on Rab5 (Fig. 4) and preferentially interacts with the GTP-bound activated form of the small GTPase (Fig. 5). These RIN2 properties are somewhat intriguing, because other identified GEFs for Rab5 including RIN1 have been reported to interact with the GDP form (21, 32). However, such

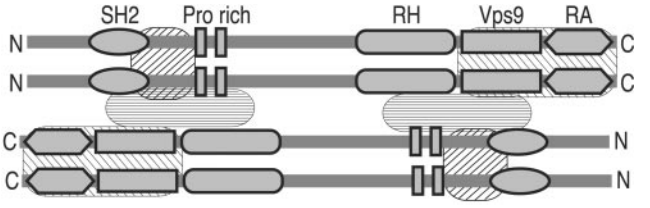

FIG. 9. **Possible model of the RIN2 tetrameric structure.** Schematic view of the RIN2 tetramer inferred from the present experiments. *Right-hatched areas* represent the amino-terminal self-interaction of RIN2. *Left-hatched areas* represent the carboxyl-terminal interaction, and *horizontally striped areas* represent the amino- and carboxyl-terminal cross-interaction.

RIN2-like properties have been also observed in a complex of Rabex-5 and Rabaptin-5. Rabex-5, previously identified as other Rab5-GEF (22), forms a tight complex with Rabaptin-5, which specifically interacts with GTP-Rab5 to stabilize its activated form (26, 46). Rabaptin-5 forms a homodimer in the multicomplex (42), and the complex formation between Rabaptin-5 and Rabex-5 is essentially required for endosome fusion (47). Thus, the unique properties of RIN2 found here may resemble to that of the Rabaptin-5-Rabex-5 complex.

The unique properties of RIN2 may be responsible for the amplification of Rab5-mediated signaling. In the endocytic pathway, RIN2 would translocate to a particular subcellular compartment by its association with the GTP form of Rab5 and catalyze re-activation of the inactivated GDP form, thereby causing the amplification of cellular responses induced by the small GTPase. Such a mechanism has been found previously (48, 49) in another GEF for the small GTPase Rap1, RA-GEF. Alternatively, the properties of RIN2 may suggest that it functions not only as an upstream GEF but also as a downstream effector for Rab5. This idea could be supported by our present data. The acceleration of nucleotide exchange reached maximum within a few minutes, and further incubation did not stimulate the exchange reaction (Fig. 5*B*). Such features of RIN2 may be explicable by its nucleotide preference for GTP-bound Rab5. We speculate that RIN2, which accomplished the nucleotide exchange on Rab5, was subsequently bound to the activated Rab5, leading to the formation of a tight ternary complex (GTP-Rab5b-RIN2). Consequently, other GDP-Rab5 molecules that remained in the reaction mixture were unable to associate with RIN2. Thus, it is likely that RIN2 may function to Rab5 stoichiometrically rather than catalytically. In the present study, we have not investigated whether the RIN2 region responsible for the GEF activity is distinguishable from the binding site for GTP-Rab5. Furthermore, we could not precisely estimate the integrity and protein stability of RIN2 used in the GEF assay, because it was immunologically purified from transfected HeLa cells. Further experiments under well established conditions should be required for clarifying these points.

Tall *et al.* (32) recently reported that RIN1 enhances its guanine exchange activity on Rab5 by its interaction with Ha-Ras. Although the direct interaction between RIN2 and Ha-Ras was not observed in the present yeast two-hybrid system, we cannot totally rule out the possibility that the GEF activity of RIN2 may be stimulated by a certain member of the Ras family other than Ha-Ras. Alternatively, the GEF function of RIN2 would be regulated by receptor-mediated signaling, because this GEF contains SH2 and Pro-rich domains, which are capable of interacting with a Tyr-phosphorylated sequence and SH3 domain, respectively. Further investigation would be also required for revealing the cross-talk between the cell signaling and the membrane trafficking.

Acknowledgment—We are grateful to Dr. David W. Russell for generous gifts of pCMV5 vector.

REFERENCES

1. Zerial, M., and McBride, H. (2001) *Nat. Rev. Mol. Cell. Biol.* **2,** 107–117
2. Wickner, W., and Haas, A. (2000) *Annu. Rev. Biochem.* **69,** 247–275
3. Waters, M. G., and Pfeffer, S. R. (1999) *Curr. Opin. Cell Biol.* **11,** 453–459
4. Novick, P., and Zerial, M. (1997) *Curr. Opin. Cell Biol.* **9,** 496–504
5. Somsel Rodman, J., and Wandinger-Ness, A. (2000) *J. Cell Sci.* **113,** 183–192
6. Meresse, S., Gorvel, J. P., and Chavrier, P. (1995) *J. Cell Sci.* **108,** 3349–3358
7. Feng, Y., Press, B., and Wandinger-Ness, A. (1995) *J. Cell Biol.* **131,** 1435–1452
8. Ullrich, O., Reinsch, S., Urbe, S., Zerial, M., and Parton, R. G. (1996) *J. Cell Biol.* **135,** 913–924
9. Lombardi, D., Soldati, T., Riederer, M. A., Goda, Y., Zerial, M., and Pfeffer, S. R. (1993) *EMBO J.* **12,** 677–682
10. Gorvel, J. P., Chavrier, P., Zerial, M., and Gruenberg, J. (1991) *Cell* **64,** 915–925
11. Van der Sluijs, P., Hull, M., Webster, P., Male, P., Goud, B., and Mellman, I. (1992) *Cell* **70,** 729–740
12. Van der Sluijs, P., Hull, M., Zahraoui, A., Tavitian, A., Goud, B., and Mellman, I. (1991) *Proc. Natl. Acad. Sci. U. S. A.* **88,** 6313–6317
13. Bucci, C., Parton, R. G., Mather, I. H., Stunnenberg, H., Simons, K., Hoflack, B., and Zerial, M. (1992) *Cell* **70,** 715–728
14. Ullrich, O., Stenmark, H., Alexandrov, K., Huber, L. A., Kaibuchi, K., Sasaki, T., Takai, Y., and Zerial, M. (1993) *J. Biol. Chem.* **268,** 18143–18150
15. Araki, S., Kikuchi, A., Hata, Y., Isomura, M., and Takai, Y. (1990) *J. Biol. Chem.* **265,** 13007–13015
16. Sasaki, T., Kikuchi, A., Araki, S., Hata, Y., Isomura, M., Kuroda, S., and Takai, Y. (1990) *J. Biol. Chem.* **265,** 2333–2337
17. Stenmark, H., Parton, R. G., Steele-Mortimer, O., Lutcke, A., Gruenberg, J., and Zerial, M. (1994) *EMBO J.* **13,** 1287–1296
18. Cavalli, V., Vilbois, F., Corti, M., Marcote, M. J., Tamura, K., Karin, M., Arkinstall, S., and Gruenberg, J. (2001) *Mol. Cell* **7,** 421–432
19. Dirac-Svejstrup, A. B., Sumizawa, T., and Pfeffer, S. R. (1997) *EMBO J.* **16,** 465–472
20. Hoffenberg, S., Liu, X., Nikolova, L., Hall, H. S., Dai, W., Baughn, R. E., Dickey, B. F., Barbieri, M. A., Aballay, A., Stahl, P. D., and Knoll, B. J. (2000) *J. Biol. Chem.* **275,** 24661–24669
21. Hama, H., Tall, G. G., and Horazdovsky, B. F. (1999) *J. Biol. Chem.* **274,** 15284–15291
22. Horiuchi, H., Lippe, R., McBride, H. M., Rubino, M., Woodman, P., Stenmark, H., Rybin, V., Wilm, M., Ashman, K., Mann, M., and Zerial, M. (1997) *Cell* **90,** 1149–1159
23. Kurosu, H., and Katada, T. (2001) *J. Biochem.* (*Tokyo*) **130,** 73–78
24. Christoforidis, S., Miaczynska, M., Ashman, K., Wilm, M., Zhao, L., Yip, S. C., Waterfield, M. D., Backer, J. M., and Zerial, M. (1999) *Nat. Cell Biol.* **1,** 249–252
25. Nielsen, E., Christoforidis, S., Uttenweiler-Joseph, S., Miaczynska, M., Dewitte, F., Wilm, M., Hoflack, B., and Zerial, M. (2000) *J. Cell Biol.* **151,** 601–612
26. Stenmark, H., Vitale, G., Ullrich, O., and Zerial, M. (1995) *Cell* **83,** 423–432
27. Gournier, H., Stenmark, H., Rybin, V., Lippe, R., and Zerial, M. (1998) *EMBO J.* **17,** 1930–1940
28. Barbieri, M. A., Roberts, R. L., Gumusboga, A., Highfield, H., Alvarez-Dominguez, C., Wells, A., and Stahl, P. D. (2000) *J. Cell Biol.* **151,** 539–550
29. Seachrist, J. L., Anborgh, P. H., and Ferguson, S. S. (2000) *J. Biol. Chem.* **275,** 27221–27228
30. McLauchlan, H., Newell, J., Morrice, N., Osborne, A., West, M., and Smythe, E. (1998) *Curr. Biol.* **8,** 34–45
31. Nielsen, E., Severin, F., Backer, J. M., Hyman, A. A., and Zerial, M. (1999) *Nat. Cell Biol.* **1,** 376–382
32. Tall, G. G., Barbieri, M. A., Stahl, P. D., and Horazdovsky, B. F. (2001) *Dev. Cell* **1,** 73–82
33. Fields, S., and Song, O. (1989) *Nature* **340,** 245–246
34. Hoshino, S., Imai, M., Mizutani, M., Kikuchi, Y., Hanaoka, F., Ui, M., and Katada, T. (1998) *J. Biol. Chem.* **273,** 22254–22259
35. Finkelstein, D. B., and Strausberg, S. (1983) *Mol. Cell. Biol.* **3,** 1625–1633
36. Horiuchi, H., Ullrich, O., Bucci, C., and Zerial, M. (1995) *Methods Enzymol.* **257,** 9–15
37. Han, L., and Colicelli, J. (1995) *Mol. Cell. Biol.* **15,** 1318–1323
38. Colicelli, J., Nicolette, C., Birchmeier, C., Rodgers, L., Riggs, M., and Wigler, M. (1991) *Proc. Natl. Acad. Sci. U. S. A.* **88,** 2913–2917
39. Han, L., Wong, D., Dhaka, A., Afar, D., White, M., Xie, W., Herschman, H., Witte, O., and Colicelli, J. (1997) *Proc. Natl. Acad. Sci. U. S. A.* **94,** 4954–4959
40. Cupers, P., ter Haar, E., Boll, W., and Kirchhausen, T. (1997) *J. Biol. Chem.* **272,** 33430–33434
41. Tebar, F., Confalonieri, S., Carter, R. E., Di Fiore, P. P., and Sorkin, A. (1997) *J. Biol. Chem.* **272,** 15413–15418
42. Vitale, G., Rybin, V., Christoforidis, S., Thornqvist, P., McCaffrey, M., Stenmark, H., and Zerial, M. (1998) *EMBO J.* **17,** 1941–1951
43. Callaghan, J., Simonsen, A., Gaullier, J. M., Toh, B. H., and Stenmark, H. (1999) *Biochem. J.* **338,** 539–543
44. Daitoku, H., Isida, J., Fujiwara, K., Nakajima, T., and Fukamizu, A. (2001) *Int. J. Mol. Med.* **8,** 397–404
45. McBride, H. M., Rybin, V., Murphy, C., Giner, A., Teasdale, R., and Zerial, M. (1999) *Cell* **98,** 377–386
46. Rybin, V., Ullrich, O., Rubino, M., Alexandrov, K., Simon, I., Seabra, M. C., Goody, R., and Zerial, M. (1996) *Nature* **383,** 266–269
47. Lippe, R., Miaczynska, M., Rybin, V., Runge, A., and Zerial, M. (2001) *Mol. Biol. Cell* **12,** 2219–2228
48. Liao, Y., Satoh, T., Gao, X., Jin, T. G., Hu, C. D., and Kataoka, T. (2001) *J. Biol. Chem.* **276,** 28478–28483
49. Liao, Y., Kariya, K., Hu, C. D., Shibatohge, M., Goshima, M., Okada, T., Watari, Y., Gao, X., Jin, T. G., Yamawaki-Kataoka, Y., and Kataoka, T. (1999) *J. Biol. Chem.* **274,** 37815–37820